

Displacement Damage induced catastrophic second breakdown in silicon carbide Schottky power diodes

Leif Scheick, *Member, IEEE*, Luis Selva, Heidi Becker

Abstract—A novel catastrophic breakdown mode in reversed biased Silicon carbide diodes has been seen for low LET particles. These particles are too low in LET to induce SEB, however SEB was seen from particles of higher LET. The low LET mechanism correlates with second breakdown in diodes due to increase leakage and assisted charge injection from incident particles. Percolation theory was used to predict some basic responses of the devices, but the inherent reliability issue with silicon carbide have proven challenging.

I. INTRODUCTION

Silicon carbide devices are becoming more attractive for harsh environments due to the inherent toughness of the silicon carbide substrate. The wide band gap of silicon carbide allows for operation of devices at high voltages and high temperature. The wide band gap also gives silicon carbide a good resistance to lattice damage, especially from displacement damage. Also, the wide band gap of silicon carbide corresponds to unique optical properties. For instance, 4H-SiC has a band gap energy of 3.26 eV and 6H-SiC has a band gap energy of 3.03. In comparison, GaAs has a band gap energy of 1.43 eV and Si has a band gap energy of 1.12 eV. Due to the wide energy band gap, silicon carbide devices can operate at extremely high temperatures without intrinsic conduction effects. Table 1 compares these and other material properties.

Silicon carbide can endure an electric field about eight times greater than Si or GaAs before exhibiting avalanche breakdown. High breakdown electric fields allow very high-voltage, high-power devices such as diodes. Also, it allows the devices to be scaled aggressively, providing ULSI options for integrated circuits. Silicon carbide has a high thermal conductivity. Heat will flow freely through silicon carbide than other semiconductor materials including metal at room temperature. This property allows extremely high power level operation and sinks the heat generated.

Silicon carbide devices are used in a wide variety of applications and have been studied for radiation and reliability in a wide spectrum of environments [1]-[3]. The innate

¹ The research in this paper was carried out at the Jet Propulsion Laboratory, California Institute of Technology under contract with the National Aeronautics and Space Administration (NASA) Code AE, under the Electronic Parts and Packaging Program (NEPP).

L. Scheick is with the Jet Propulsion Laboratory, California Institute of Technology, Pasadena, CA 91109 USA (telephone: 818-354-3272, e-mail: leif.scheick@jpl.nasa.gov).

H. Becker is with the Jet Propulsion Laboratory, California Institute of Technology, Pasadena, CA 91109 USA (telephone: 818-354-3272, e-mail: heidi.becker@jpl.nasa.gov).

L. Selva is with the Jet Propulsion Laboratory, California Institute of Technology, Pasadena, CA 91109 USA (telephone: 818-354-3272, e-mail: luis.selva@jpl.nasa.gov).

robustness of silicon carbide gives it a high breakdown voltage and resistance to stress induced breakdown [4]-[7]. Silicon carbide has also recently been studied for total ionizing and displacement damage effects [8]-[12]. Silicon carbide has shown innate hardness to displacement damaging and ionizing radiation. Discrete silicon carbide devices have shown a similar robustness in performance during and after irradiation.

TABLE I.
COMPARISON OF SEMICONDUCTOR PARAMETERS.

	4H-SiC	6H-SiC	GaAs	Si
Band gap energy [eV]	3.26	3.03	1.43	1.12
Breakdown electric field [V/cm]	2.20E+06	2.40E+06	3.00E+05	2.40E+05
Thermal Conductivity [W/cm K @ RT]	3.45	3.45	0.5	1.5
Saturates electron drift velocity [cm/sec (@ E 2 x 10 ⁵ V/cm)]	2.00E+07	2.00E+07	1.00E+07	1.00E+07

This paper presents and discusses catastrophic failure modes in silicon carbide power diodes due to proton and heavy ion radiation that contradicts that current body of results. These results also defy the expectations of the silicon carbide design.

II. THEORY

Silicon carbide can experience burnout due to defects in the lattice. Screw plane defects can cause microfilaments that lead to device breakdown. Silicon carbide lattices continue to suffer from a variety of defect producing impurities [13]. Large screw defects, with Burg vectors over two lattice sites, are called micro-pipes and are a major failure mode in silicon carbide substrates [13], [14]. Breakdown characteristics continue to be a limiting factor in Silicon carbide devices [13]. One reason for this weakness is defects in Silicon carbide tend to be much more conductive than in Si. Micropipes are especially troublesome since the interior of the structure has a high conductivity. Silicon carbide also has a more propensity to negative temperature coefficient breakdown in the presence of defects.

Silicon and silicon carbide have a 20% lattice mismatch. The transition from silicon to silicon carbide can cause defects and stresses on the substrate [15]. Also, silicon carbide exhibit "polytypism," which makes fabrication and process control a uniquely hard challenge for silicon carbide devices. Multiple types in a substrate can lead to plane, point and screw defects in a substrate [7], [13]. These defects decrease the breakdown performance of the silicon carbide. Neutron irradiation has been shown to induce defects in silicon carbide substrates [15]. Phase change amorphization has been caused by intense electron radiation, with defects increasing at lower fluences [16].

Figure 1 juxtaposes a pn diode structure and a Schottky diode structure. The primary difference is the rectifying structure in the pn diode is the pn junction, while the Schottky diode uses a metal semiconductor contact as the rectifying junction. The breakdown characteristics are

essentially the same for pn and Schottky diodes. Schottky silicon diodes do have lower breakdown voltages compared to silicon pn diodes due to high curvature in depletion region layers, silicon surface effects, and ohmic contact issues [4], [5], [6]. Device architecture can compensate for some of the weaknesses of Schottky structures. Silicon carbide's wide band gap, and therefore higher breakdown voltage, allows for a more robust Schottky device.

Silicon carbide Schottky diodes have been available commercially for some time. Schottky diodes have been shown to be simple to manufacture and the silicon carbide substrate has been shown to integrate most easily with the Schottky architecture. Silicon carbide's unique lattice structure allows for an equally unique doping structure. Boron doping takes a carbon site and aluminum takes the silicon site. This characteristic allow for compensated doping and more defined intrinsic regions [4]- [6]. Silicon carbide has exhibited several reliability problems that have seriously impacted yield. Figure 2, taken from [18], plots the distribution of breakdown voltages of virgin Schottky barrier diodes. These diodes were free of micropipe defects, which are major failure cause in Silicon carbide. Lesser defects would be present and presumably contribute to the defects.

All diodes exhibit a high current, low voltage condition after avalanche breakdown that is related to the thermal breakdown of the device. This is called second breakdown or snap back. The second breakdown condition onsets when the intrinsic carrier concentration, n_i , is equal to the dopant concentration, N_d [19], or

$$n_i = N_d \text{ and} \quad (1)$$

$$n_i = \sqrt{N_c N_v} e^{\frac{-E_g}{kT}} \quad (2)$$

where N_d is the dopant density, N_c is the effective electron density of states in the conduction band, and N_v is the effective density of states in the valence band. Obviously from (2), high temp in a local region, whether cause by ions and/or defects will trigger second breakdown. Defects have been linked to the formation of microplasmas that can trigger a temperature rise that instigates second breakdown [18]. Essentially, this condition equates to a high power density rise, or:

$$P_D = \sqrt{\pi \kappa \rho C_p} (T_m - T_i)^{-1/2} \quad (3)$$

where P_D is the power density, κ is the thermal conductivity, ρ is the density, C_p is the specific heat, T_m is failure temperature, and T_i is the initial temperature [14]. Eq. (3) is especially important for this study as the micro-plasma of an ion strike occurs on a very small time scale. Both bulk and screw defects have been linked with increased breakdown in silicon carbide devices [7]. Eq. (3) is unique in that, in contrast to (1) and (2), none of the parameters in (3) should be largely affected by radiation. N_d , N_c , and N_v in (1) and (2) are sensitive to displacement damage. Eq. (3) is relevant though as it is still the condition in which a microplasm will trigger on defects.

Silicon diodes experience the breakdown described by (1), (2), and (3). In general, these devices will experience the aforementioned breakdown at very high reverse biases or under irradiation from high LET ($>20 \text{ MeV.cm}^2/\text{mg}$) ions. Proton irradiation in silicon diode structures usually follows the behavior shown in Fig. 3. Reverse bias leakage current monotonically increases with fluences due to defects in the devices. No prompt failures are seen since the effective LET of a proton induced spallation reactions are not high enough to induce SEB. The failure mode is simply overwhelming leakage current.

Silicon carbide reversed bias junction under displacement damage inducing radiation will exhibit an increase in defects. The same irradiation should cause rare energy depositions that construct the microplasmas that trigger the condition in (3). Second breakdown results in catastrophic destruction of the device, much like SEB. The displacement damage causes the defects that increase leakage and temperature and setup micro-plasmas, and the rare energy events inject the current required to trigger the second breakdown as described in (3). This effect should occur only under the conditions of high voltage, to setup the microplasma transport, low LET, as high LET will cause SEB immediately, and a critically high defect population caused by displacement damage. This condition is mathematically described by percolation theory, which is mainly used in the description of breakdown in thin oxides in VLSI and ULSI devices [20]-[24].

Percolation theory in SiO_2 is similar to the reverse biased diode in that both have a clearly segregated energy bands. The oxide is such due to the insulator nature of the oxide and the diode to the reverse bias field [20],[22]. Figure 4 portrays a possible condition for an ion assisted percolation failure of a device. After enough defects are induces by ions to almost make a circuit, a rare energy deposition from a proton completes the circuit and provides enough liberated carriers to prime to circuit and initiate negative temperature coefficient breakdown. Since the percolation circuits also contains pre-irradiation defects like micropipes. These defects will reduce the number of radiation-induced defects required to complete the percolation circuit. Figure 5 demonstrates this theory. The current should rise with fluence at a constant reverse bias voltage, which is region 1. Region two is after a 2nd break down occurs in the device due to increased defect population, enhancing microplasma injection from light ions to form the burnout path.

The first order percolation theory reveals a useful prediction to breakdown damage levels even with the large noise margins that Silicon carbide device seem to have. Starting with:

$$N_d = N_{d0} (1 - e^{-\sigma_i \Phi}) \quad (4)$$

which is a statement of the generation rate of defects in the active region. N_d is the number of defects, N_{d0} is the maximum number of defects, and σ_i is the cross section for defect placement in the active region. Since the overall microplasma path is long, the actual number of defects required for burnout is expected to be low so this approximation applies:

$$N_d = N_{d0} \sigma_t \Phi . \quad (5)$$

Percolation theory predicts breakdown will occur when a circuit of defects supplies a path for microplasma from an ion to be supported with a negative temperature coefficient. This statement is essentially

$$V_{BD} = C (r_d^{ave})^\alpha , \quad (6)$$

where V_{BD} is the breakdown voltage, C and α are constants, and r_d^{ave} is the average distance between defects. The average defect distance is related to the defect number by:

$$\frac{N_d}{N_{d0}} = \left(\frac{d_{SiC}}{r_d^{ave}} \right)^3 \quad (7)$$

where d_{SiC} is the lattice constant for Silicon carbide. Combining (5) and (7) yields,

$$r_d^{ave} = d_{SiC} \left(\frac{1}{\sigma_t \Phi} \right)^{\frac{1}{3}} . \quad (8)$$

Plugging (8) into (6) then yields,

$$V_{BD} = C \left(\frac{d_{SiC}^3}{\sigma_t \Phi} \right)^{\frac{\alpha}{3}} . \quad (9)$$

The constants C and α will depend heavily on parameters such as dopant gradation, contact architecture and initial defect density. The acquiring of these and other obscure and privileged information was out of the scope of this study. Eq. (9) should apply to both biased and unbiased irradiation, but the constant will change to accommodate the different average defect distance. The dependence is where (1), (2), and (3) change the r_d^{ave} value. Charge injection from rare and large energy proton events effectively reduce the average defect distance required for the microplasma event.

SEB should immediately be seen for high LET particles. The amount of charge injected by a high LET ion will immediately cause a microfilament type structure that leads to SEB. The transition from the low LET behavior to high LET behavior should indicate diode parameters. Therefore, reversed biased silicon carbide diodes should be seen to experience a SEB like breakdown under irradiation with high LET ions and experience a second breakdown event after a critical amount of irradiation.

III. PROCEDURE AND SETUP

The parts selected for this were silicon carbide diodes from Cree, Inc. The CSD01060 and CSD04060 are the part numbers. These are Schottky diodes that are available commercially. Nitrogen is used to dope the device to n-type while the aluminum is used to dope to p-type.

For the primary measurement method, an HP4142 modular semiconductor measurement system was used with a 200 volt module (HP41420A), connected to the anode, and a single 1000 volt module (HP 411423A) was connected to the cathode. The HP4142 was connected to and controlled by a computer via a general-purpose instrument bus (GPIB). The devices were tested electrically for electrical breakdown (in a

non-destructive test) prior to irradiation using the test equipment and setup. Electrical breakdown was defined as the voltage where the collector current (I_C) reached the current limit of 10^{-3} A. When the device under test (DUT) reached this current limit, the applied voltage was removed within 10^{-3} seconds, allowing multiple measurements of the DUT. All electrical measurements were performed using the HP4142 source modular unit (SMU). Prior to irradiation all devices were characterized for forward voltage (V_f) and leakage current (I_{AC}) from anode to cathode.

To ensure that the testing method was not a factor in the breakdown of the device, a manual system was employed for a significant fraction of the proton testing. A discrete 1000V power supply was used to force a reverse bias while a DMM was used to measure leakage current. The leakage current could be measured by hand or capture through and RS-232 interface. All of the test fixtures were likewise changed in design to further remove experimental setup as a factor.

The SEU test facilities at BNL provided a wide range of ions and energies for SEE testing. The Crocker Nuclear Laboratory (CNL) of the University of California at Davis (UCD) has developed a facility to test radiation effects on photonic and electronic devices. The facility provides proton, deuteron and He-4 (alpha-particle) beams up to 68, 45, 90MeV respectively. Beam fluxes depend of the degree of uniformity needed at the Device Under Test (DUT) location. A list of ions used in this study is shown in Table 2.

TABLE 2.
IONS USED IN THIS STUDY.

Ion @ Energy	LET (MeV cm ² /mg)	Facility	Range in Si (microns)
Protons @ 67.5 MeV	0.01	CNL	>1000
Lithium @ 99MeV	0.37	BNL	306
Fluorine @ 125 MeV	3.634	BNL	102
Bromine @ 210MeV	36	BNL	63.5
Iodine @ 329MeV	59.8	BNL	31.6

IV. RESULTS

The diodes tested demonstrated the expected response somewhat. High LET particles induce SEB at very low fractions of the rated reverse breakdown voltage. Low LET particles degraded the parts until prompt failure identical in signature to second breakdown, i.e., high current and low voltage. Both of the methods of employing the HP4142 and the manual method had equivalent results. For fluences lower than 10^{15} cm⁻², breakdown did not occur for devices irradiated unbiased or biases lower than 400V when brought up to full rated reverse bias, or 600V. This implies that the breakdown mechanism is due to the proton induce events coupled with a damaged oxide.

Figure 6 compares well with the conceptual prediction of Figure 5. The device experiences a catastrophic breakdown after a smaller increase in the current. The current was limited by the HP4142. The device did not show a steady

increase in current below the small jump at $7 \times 10^{11} \text{ cm}^{-2}$. Current density may require a critical dose to increase significantly. Several devices have shown a critical dose response [25], [26]. The jump in current before catastrophic failure is an anomaly. Most devices do not notably change in current from proton irradiation. Figure 7 shows a typical set of devices measured to relate the fluence required to induce breakdown and the voltage at which breakdown occurs. Of eight devices, one was irradiated at 600V reverse bias (Fig. 7a), three were irradiated at 500V (Fig. 500V), and four were irradiated at 550V (550V). From these plots, the extreme variance in device parameters and response can be seen. Initial leakage current, slope of current increase with fluence, and the fluence at which breakdown occurs all have wide variation. This is not surprising considering the results shown in Fig. 2.

Figure 8 compares the initial leakage currents at 600V reverse bias for all of the devices tested in this study. Note that the abscissa is a log axis, which is due to three orders of magnitude range in the values. There is no clear behavior to the distribution. The values were persistent between measurements. To determine whether initial current correlates to breakdown voltage induced by radiation, the initial current and radiation induce breakdown fluence are plotted on Fig. 9. Figure 9a shows the response in linear-linear scale, while Fig 9a. shows the log-linear response. No clear trend can be seen between initial current and breakdown fluence can be seen. Both responses the irradiations at 500V and 600V are plotted. A relation between breakdown voltage and breakdown fluence can be seen though. Devices irradiated at 600V breakdown at fluences one order of magnitude less than devices irradiated at 500V. The relation between breakdown voltage and breakdown fluence is plotted in Fig. 10. Most of the devices biased at 400V didn't breakdown, so the 400V point in Fig. 10 is a lower bound. This response agrees with the prediction of (9). Due to the wide variation of breakdown voltages observed, the errors bars in Fig. 10 are wide. The error bars in Fig. 10 are one standard deviation. The bars are too wide to allow a confident extraction of the alpha constant. The behavior of Fig. 10 does agree well with (9).

The devices irradiated with ions with LETs over 10 MeV.cm²/mg induce a rapid SEB response. Figure 11 shows the relation between LET and the breakdown voltage. The same data with NIEL on the abscissa is shown in Figure 12. There is a similar strong dependence on NIEL. This response is similar to LET response. Both responses are typical of SEB responses seen for other power devices except that the proton failure modes.

The response of breakdown voltage as a function of fluence is shown in Figure 13. Higher LET ions require less fluence to cause a breakdown event. Iodine and Bromine require less than a second of flux to cause a breakdown that is typical of SEB. This indicates that the SEB induced by heavy ions requires not pre-irradiation. Fluorine, Lithium, and protons require a significant amount of fluence to induce a breakdown event. Figure 14 depicts the breakdown voltage vs. total dose. The heavy ions are clearly segregated from the

low LET particle, which is indicative of the duality of the high LET and low LET responses.

V. CONCLUSIONS

Silicon carbide Schottky diodes have shown an unprecedented radiation sensitivity in the reverse biased condition. Silicon carbide device are normally considered to be extremely robust to displacement damage radiation, but device tested here show a unique failure mode that belies this trend.

VI. ACKNOWLEDGMENT

The authors would like to thank Mike Weideman, Dennis Thorbourne, and Tetsuo Miyahira of the Jet Propulsion Laboratory as well as Richard Harris and Martin Patton of Glenn Research Center.

VII. REFERENCES

- [1] D.Braunig; Fritsch, D.; Lehmann, B.; Barry, A.L.; Radiation-induced displacement damage in silicon carbide blue light-emitting diodes Nuclear Science, IEEE Transactions on, Volume: 39, Issue: 3, June 1992 Pages:428 - 430
- [2] McGarrity, J.M.; McLean, F.B.; DeLancey, W.M.; Palmour, J.; Carter, C.; Edmond, J.; Oakley, R.E.; Silicon carbide JFET radiation response Nuclear Science, IEEE Transactions on, Volume: 39, Issue: 6, Dec. 1992 Pages:1974 - 1981
- [3] Barry, A.L.; Lehmann, B.; Fritsch, D.; Braunig, D.; Energy dependence of electron damage and displacement threshold energy in 6H silicon carbide Nuclear Science, IEEE Transactions on, Volume: 38, Issue: 6, Dec. 1991 Pages:1111 - 1115
- [4] Ned Mohan, Tore M. Undeland, William P. Robbins. *Power electronics: converters, applications, and design*, 3rd ed. Hoboken, NJ : John Wiley & Sons, c2003. xvi
- [5] Trzynadlowski, Andrzej. *Introduction to modern power electronics*, New York : Wiley, c1998. x, 433 p. : ill. ; 24 cm.
- [6] Sen, P. C. (Paresh Chandra), Principles of electric machines and power electronics / P.C. Sen., 2nd ed. New York : John Wiley & Sons, c1997.
- [7] Neudeck, P.G.; Wei Huang; Dudley, M.; Study of bulk and elementary screw dislocation assisted reverse breakdown in low-voltage (<250 V) 4H-SiC p+-n junction diodes. I. DC properties Electron Devices, IEEE Transactions on, Volume: 46, Issue: 3, March 1999 Pages:478 - 484
- [8] Scozzie, C.J.; McGarrity, J.M.; Blackburn, J.; DeLancey, W.M.; Silicon carbide FETs for high temperature nuclear environments Nuclear Science, IEEE Transactions on, Volume: 43, Issue: 3, June 1996 Pages:1642 - 1648
- [9] McGarrity, J.M.; Scozzie, C.J.; Blackburn, J.; Delancy, W.M.; High temperature silicon carbide FETs for radiation environments Nuclear Science Symposium and Medical Imaging Conference Record, 1995, 1995 IEEE, Volume: 1, 21-28 Oct. 1995 Pages:144 - 147 vol.1
- [10] Ionascut-Nedelcescu, A.; Carlone, C.; Houdayer, A.; von Bardeleben, H.J.; Cantin, J.-L.; Raymond, S.; Radiation hardness of gallium nitride Nuclear Science, IEEE Transactions on, Volume: 49, Issue: 6, Dec. 2002 Pages:2733 - 2738
- [11] McGarrity, J.M.; McLean, F.B.; DeLancey, W.M.; Palmour, J.; Carter, C.; Edmond, J.; Oakley, R.E.; Silicon carbide JFET radiation response Nuclear Science, IEEE Transactions on, Volume: 39, Issue: 6, Dec. 1992 Pages:1974 - 1981
- [12] McLean, F.B.; McGarrity, J.M.; Scozzie, C.J.; Tipton, C.W.; DeLancey, W.M.; Analysis of neutron damage in high-temperature silicon carbide JFETs Nuclear Science, IEEE Transactions on, Volume: 41, Issue: 6, Dec 1994 Pages:1884 - 1894
- [13] Neudeck, P.G.; Fazi, C.; Study of bulk and elementary screw dislocation assisted reverse breakdown in low-voltage (<250 V) 4H-SiC p+-n junction diodes. II. Dynamic breakdown properties

- Electron Devices, IEEE Transactions on, Volume: 46, Issue: 3, March 1999 Pages:485 – 492
- [14] P. G. Neudeck, W. Huang, M. Dudley, And C. Fazi, Non-Micropipe Dislocations In 4h-Sic Devices: Electrical Properties And Device Technology Implication, MRS Symposium Proceedings Volume 512, pp. 107-112,
- [15] Nagesh, V., J.W. Farmer, R.F. Davis, and H.S. Kong. Defects in neutron irradiated SiC. Appl. Phys Lett. 50(47), 27 April 1987.
- [16] Manabu Ishimaru, In-Tae Bae, and Yoshihiko Hirotsu, Electron-beam-induced amorphization in SiC PHYSICAL REVIEW B 68, 144102 ~2003!
- [18] KAMATA
- [19] Amerasekera, A.; Chang, M.-C.; Seitchik, J.A.; Chatterjee, A.; Mayaram, K.; Chern, J.-H.; Self-heating effects in basic semiconductor structures Electron Devices, IEEE Transactions on, Volume: 40, Issue: 10, Oct. 1993 Pages:1836 – 1844
- [20] W. Kai, X. Hengkhun, and Ge. Jingpang, "Percolation and dielectric breakdown," Proceedings of the 4th International Conference on Properties and Applications of Dielectric Commercials, July 3-8, 1994, Brisbane Australia.
- [21] R. Degraeve, G. Groeseneken, R. Bellens, J. L. Ogier, M. Depas, P. J. Roussel, and Herman E. Maes, "New insights in the relation between electron trap generation and the statistical properties of oxide breakdown," *Electron Devices, IEEE Transactions On*, Vol. 45, No. 4, April 1998.
- [22] W. H. Lin, K. L. Pey, Z. Dong, S. Y. M. Chooi, C. H. Ang, and J. Z. Zheng, "The Statistical Distribution of Percolation Current for Soft Breakdown in Ultrathin Gate Oxide," 336 *IEEE Electron Device Letters*, Vol. 24, No. 5, May 2003.
- [23] M. A. Alam, B. E. Weir, P. J. Silverman, "A Study of Soft and Hard Breakdown—Part I: Analysis of Statistical Percolation Conductance," *IEEE Transactions On Electron Devices*, Vol. 49, No. 2, February 2002
- [24] S. S. Sombra, U. M.S. Costa, V. N. Freire, E.A. de Vasconcelos, E. F. da Silva Jr., "A percolation based dielectric breakdown model with randomic changes in the dielectric constant," *Physica A* 305 (2002) 351 – 359.
- [25] Ferlet-Cavrois, V.; Quoizola, S.; Musseau, O.; Flament, O.; Leray, J.L.; Pelloie, J.L.; Raynaud, C.; Faynot, O.; Total dose induced latch in short channel NMOS/SOI transistors Nuclear Science, IEEE Transactions on, Volume: 45, Issue: 6, Dec. 1998 Pages:2458 – 2466
- [26] Sexton, F.W.; Fleetwood, D.M.; Shaneyfelt, M.R.; Dodd, P.E.; Hash, G.L.; Schanwald, L.P.; Loemker, R.A.; Krisch, K.S.; Green, M.L.; Weir, B.E.; Silverman, P.J.; Precursor ion damage and angular dependence of single event gate rupture in thin oxides Nuclear Science, IEEE Transactions on, Volume: 45, Issue: 6, Dec. 1998 Pages:2509 – 2518

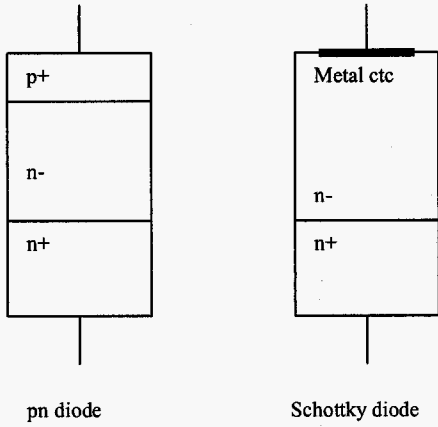


Fig. 1. PN and Schottky diode structures.

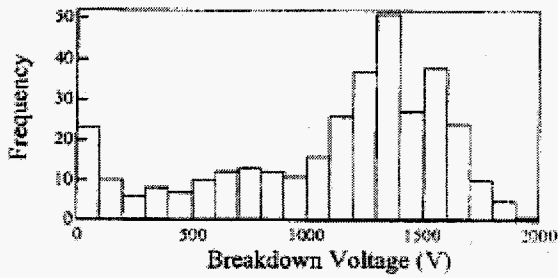


Fig. 2. Distribution of breakdown voltages in defect free Schottky barrier diodes. Taken from [A].

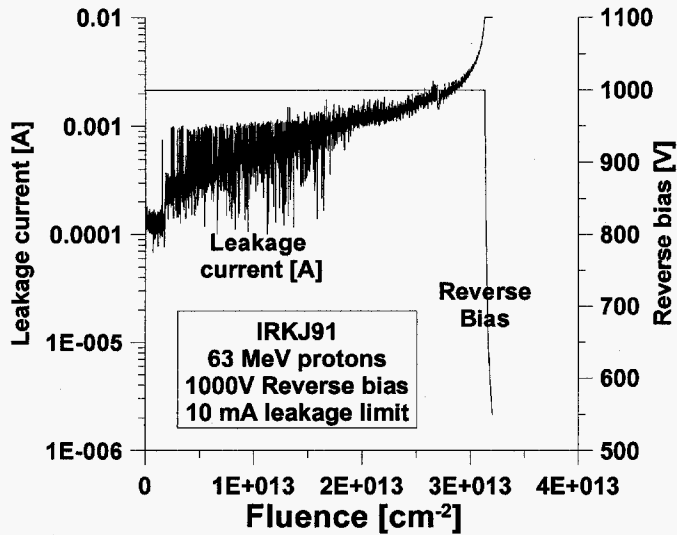


Fig. 3. Response of a silicon power diode to 63 MeV protons. The response is typical of leakage induced by defects. Leakage increase with fluence with no prompt SEE effects. Device was biased at 1000V.

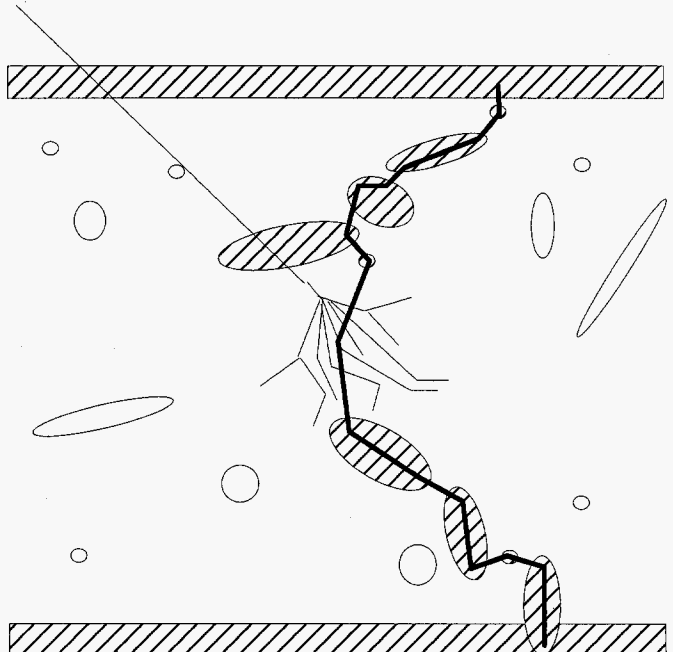


Fig. 4. Depiction of how a circuit of defects can initiate a prompt breakdown. Random injection of conductive defects is described by percolation theory. Conductive defects can be radiation defects or clusters, screw defects or micropipes, or stacking faults.

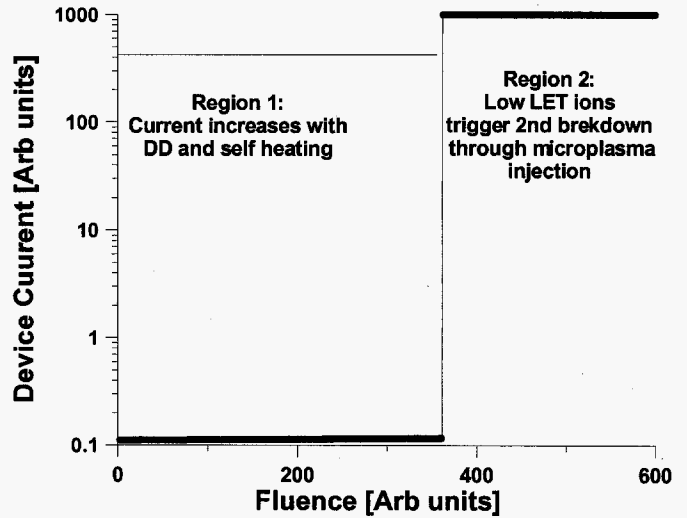


Fig. 5. Postulated response of a silicon carbide Schottky diode to light ion dose. The prompt failure is due to the completion of the percolation circuit triggered by a microplasma injection from a proton rare event. Breakdown does not occur when the device is irradiated unbiased and then biased until much higher fluences.

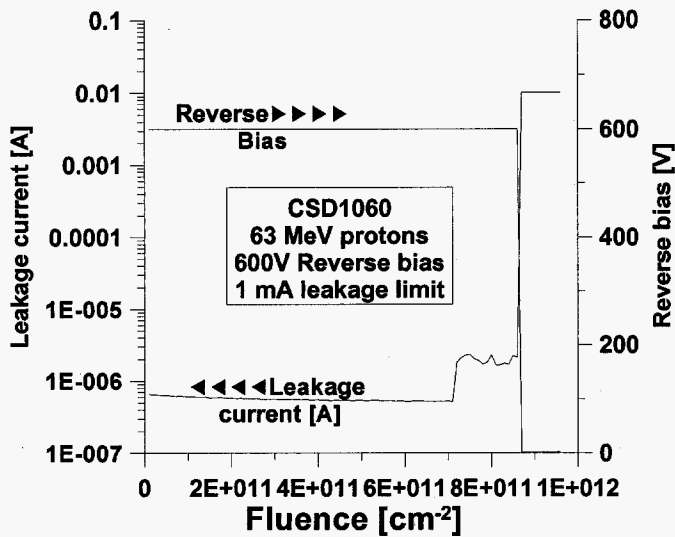


Fig. 6. Response of a silicon carbide Schottky CSD1060 diode to proton dose. Device was biased at 600V. Unlike Si devices, the leakage current down not in general increase with fluence, but actually decreases until single event type event occur.

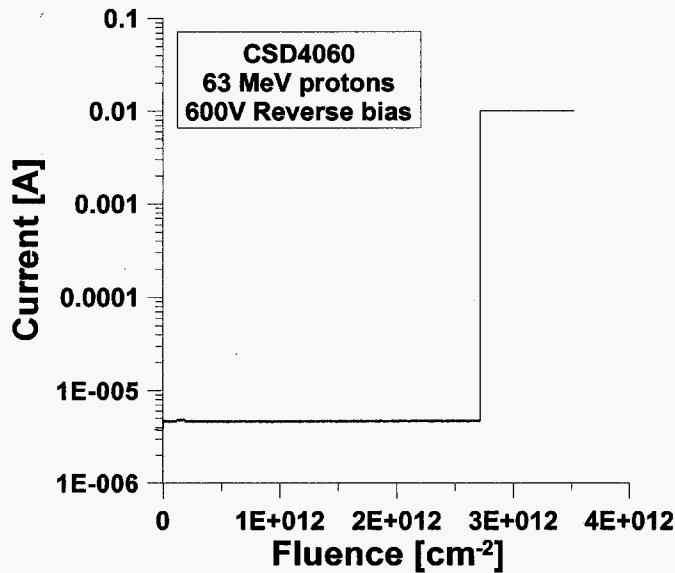


Fig. 7a. Response of a silicon carbide Schottky CSD4060 diode to proton dose. Device was biased at 600V. The leakage does not change during irradiation before the prompt failure.

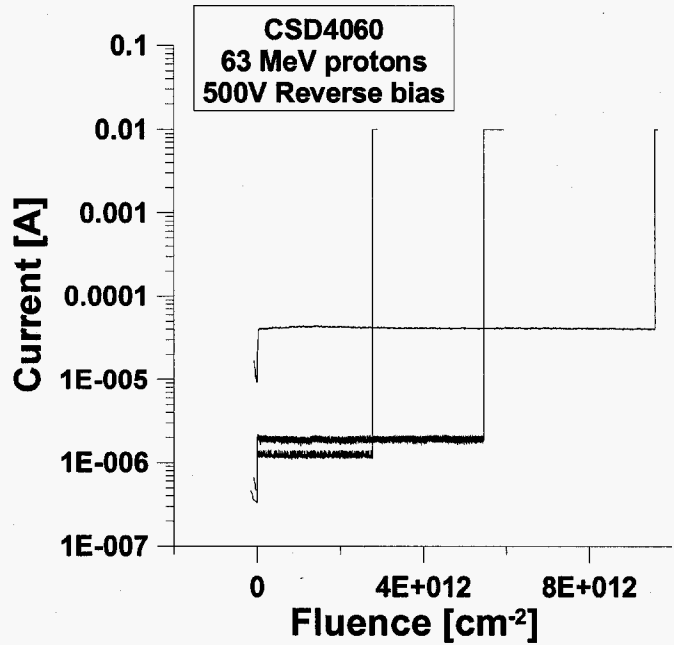


Fig. 7b. Response of a silicon carbide Schottky CSD4060 diode to proton dose. Device was biased at 500V.

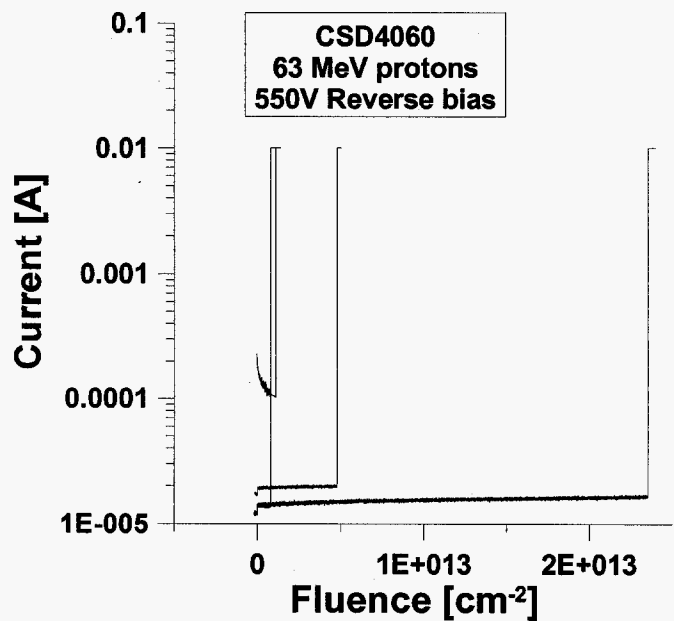


Fig. 7c. Response of a silicon carbide Schottky CSD4060 diode to proton dose. Device was biased at 550V.

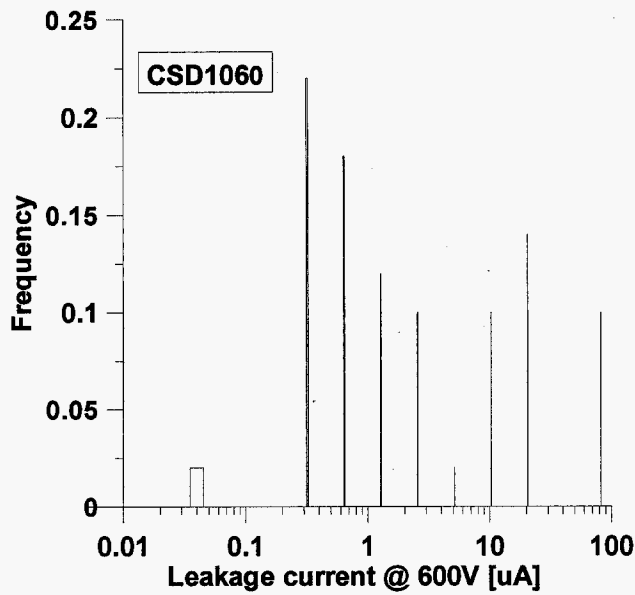


Fig. 8. Distribution of reverse bias leakage current at 600V reverse bias. The parts tested in this study experiences variance of over three orders of magnitude.

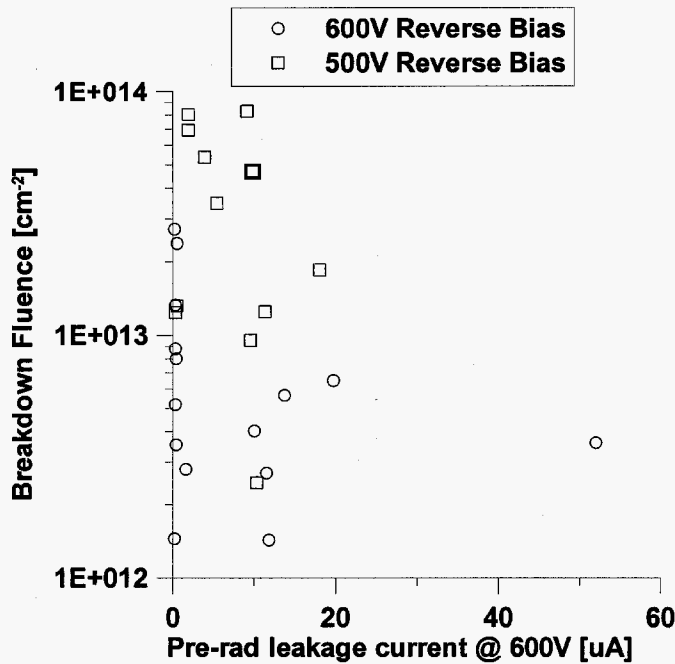


Fig. 9a. Scatter plot of the fluence at which breakdown occurred versus the pre-irradiation leakage current. No trend is obvious except that the irradiation at 600V correlated to a breakdown fluence one magnitude less than irradiations are 500V reverse bias.

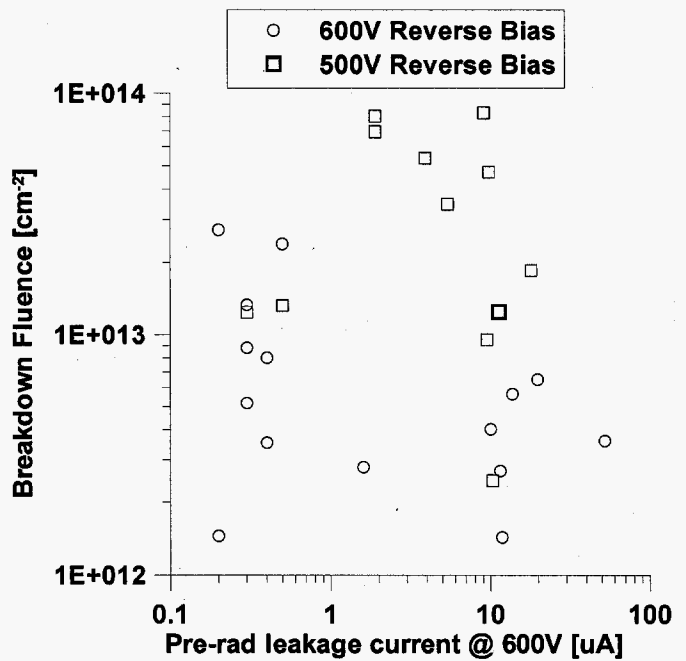


Fig. 9b. Scatter plot of the fluence at which breakdown occurred versus the pre-irradiation leakage current. No trend is obvious except that the irradiation at 600V correlated to a breakdown fluence one magnitude less than irradiations are 500V reverse bias.

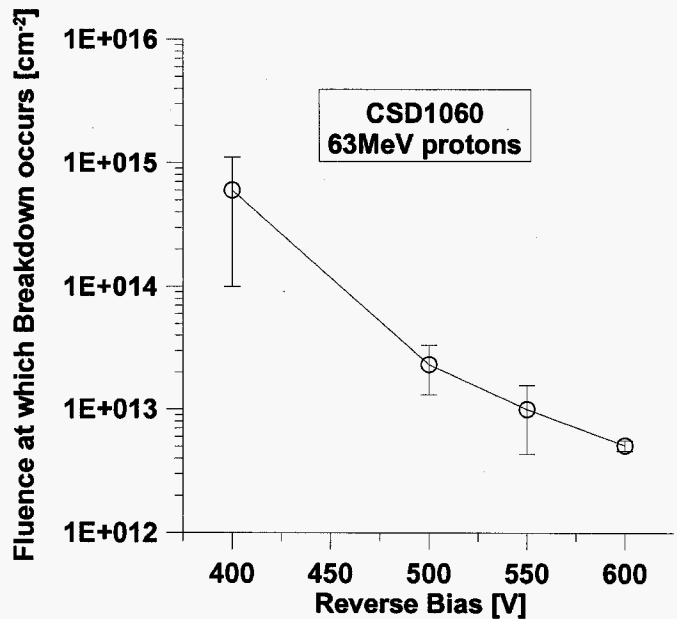


Fig. 10 Mean Fluences for Prompt Failure of csd1060 versus reverse bias voltage. Error bars are the standard deviation for fluences required for prompt failure for each bias condition. Due to the large inherent variance in the breakdown voltages of the devices, the error bars are quite large but a trend is evident.

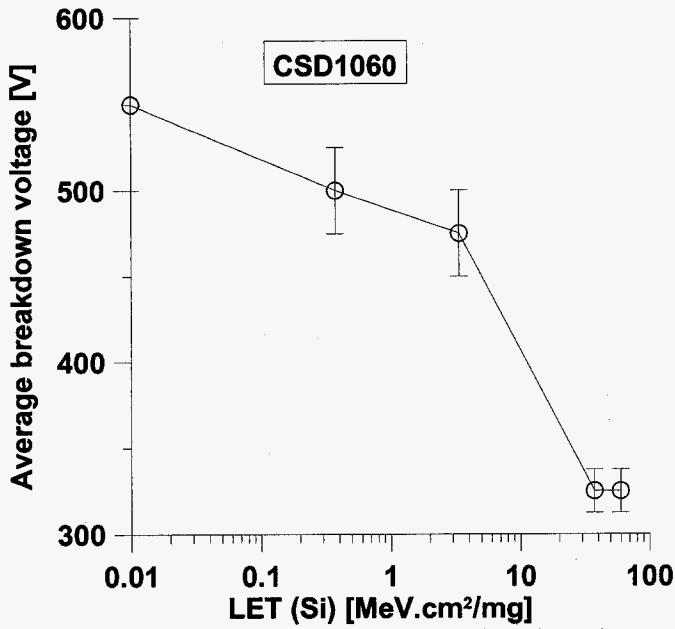


Fig. 11. Voltage at which a silicon carbide diode experience destructive breakdown as a function of LETs of different ions. The device begins to experience immediate SEE type effects at LETs over 10 MeV-cm²/mg.

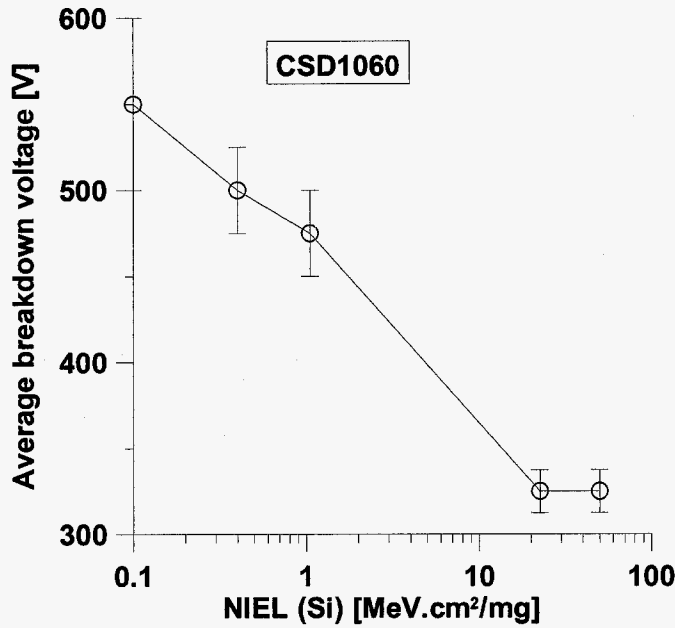


Fig. 12. Voltage at which a silicon carbide diode experience destructive breakdown as a function of NIELs of different ions. The response appears linear but the variation in fluence (not shown here) is an important variable.

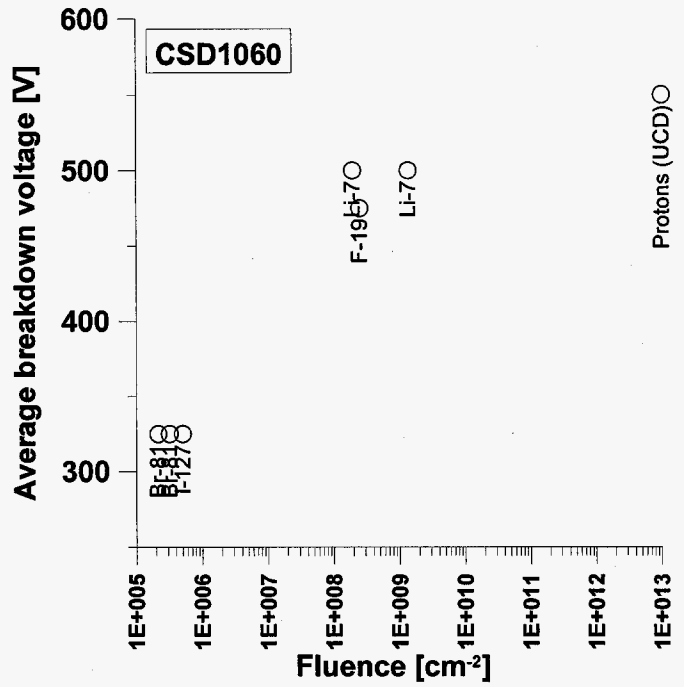


Fig. 13. Voltage at which a silicon carbide diode experience destructive breakdown as a function of particle fluence. This plot is essentially recasting of the plot shown in Fig. 11.

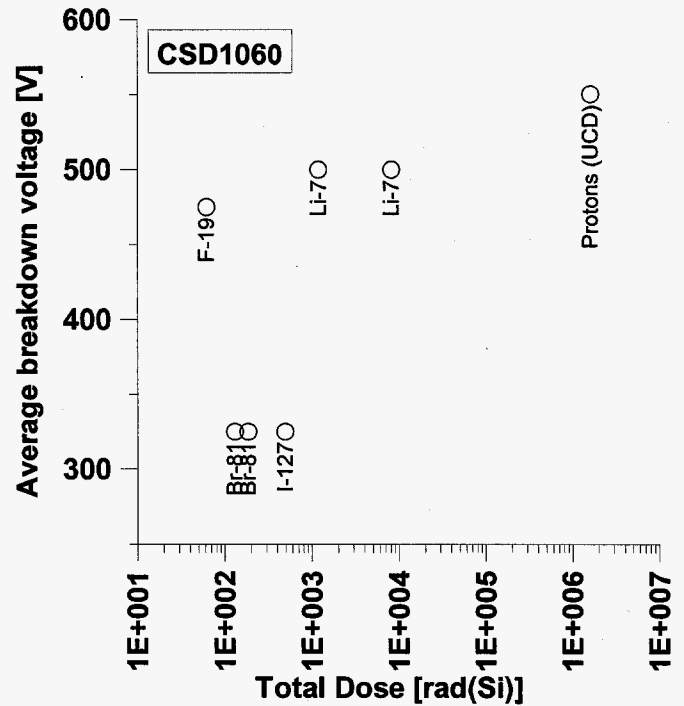


Fig. 14. Voltage at which a silicon carbide diode experience destructive breakdown as a function of dose.

End of File

